Amphiphilic ionic complexes of hyaluronic acid with organophosphonium compounds and their antimicrobial activity

Ana Gamarra [a], Eva Forés [b], Jordi Morató [b], Sebastián Muñoz-Guerra [a],*

[a] Departament d'Enginyeria Química, Universitat Politècnica de Catalunya, ETSEIB, Diagonal 647, Barcelona 08028, Spain
[b] Health and Environmental Microbiology Lab & UNESCO Chair on Sustainability, Universitat Politècnica de Catalunya, ESEIAAT, Edifici Gaia, Pg. Ernest Lluch/Rambla Sant Nebridi, Terrassa 08222, Spain

ARTICLE INFO

ABSTRACT

Amphiphilic ionic complexes of hyaluronic acid and alkyltrimethylphosphonium soaps with alkyl chains containing even numbers of carbons from 12 to 22 have been produced. The complexes have a nearly stoichiometric composition, are non-water soluble, and are stable to heat up to temperatures above 200 °C. These complexes are amphiphilic and able to adopt a biphasic structure with the paraffinic and polysaccharide phases ordered arranged with a periodicity ranging between 3 and 5 nm depending on n. The paraffinic phase in complexes with $n \geq 18$ was crystallized and showed melting at temperatures between 58 and 70 °C depending on the n value. The complexes decomposed upon incubation in water under physiological conditions, and undergone extensive biodegradation by the action of hyaluronidases. Biocide assays carried out in both solid and liquid media demonstrated a high antimicrobial activity of the complexes against Gram-positive S. aureus but moderate against Gram-negative E. coli and C. albicans fungi.

© 2018 Elsevier B.V. All rights reserved.

1. Introduction

Hyaluronic acid (HyA) is a linear polysaccharide which is ubiquitous in the human body. Its high viscoelasticity and great capacity for holding water, as well as its inherent biocompatibility and biodegradability, are properties that make HyA an outstanding biomaterial for medical and pharmaceutical applications [1,2]. Furthermore hyaluronic acid is also important in the regulation of injury associated reactions because it promotes early inflammation, which is a critical step for starting wound healing [3,4]. A number of strategies for the chemical modification of HyA addressed to improve its physicochemical properties, most of them based on the reaction of carboxyl or hydroxyl groups, have been developed [1,5,6]. A valid alternative approach for the modification of HyA is its coupling with cationic surfactants. It has been widely reported that this type of modification carried out on polyelectrolytes (either polypeptides or polyuronic acids) gives rise to stable comb-like ionically-linked systems able to self-assemble in amphiphilic structures [7,8]. These structures consist of two phases, one paraffinic and the other made of the biopolymer, that alternate in layers with a periodicity of several nanometers. Interestingly, the nanometric dimensions of such structures are reversibly responsive to thermal effects. Consequently, these derivatives are potentially useful to design medical devices with temperature-depending transport activity [9]. Additionally,

the convenience of nanostructured polymeric systems as antimicrobial materials has been recently featured [10].

According to what has been noticed in a recent investigation, HyA is able to exert bacteriostatic effects and also to display antimicrobial and antiviral properties [11,12]. However, as it has been reported by a number of authors, the biocide effect of this polysaccharide is not clear, and it seems to critically depend on its molecular weight and its concentration in solution. It is therefore advisable that HyA is used in combination with well recognized antimicrobial agents in order to avoid such dependences and ensure its bacteriostatic effect. Nisin, silver and polyhexanide are among others, active compounds that have been added to HyA to make it an efficient antimicrobial system [13–15].

In this study tetraalkylphosphonium surfactants have been coupled to HyA to generate stable ionic complexes with comb-like architecture and antimicrobial properties. The biocide activity of quaternary-onium salts has been widely demonstrated [16], and organophosphonium salts are particularly efficient in this regard [17]. In fact, these compounds have been extensively used in the preparation of polymeric materials with remarkable antimicrobial activity [18–21]. Furthermore organo-phosphonium compounds are known to be much more resistant to temperature than their organo-ammonium analogs [22]. In this work, alkyltrimethylphosphonium bromide soaps, abbreviated as nATMP·Br, with n standing for the number of carbon atoms contained in the linear alkyl chain and taking even values from 12 to 22, have been coupled with HyA to give the ionic nATMP·HyA complexes. The study is parallel to those recently published by us on the ionic complexes of HyA with

* Corresponding author.
E-mail address: sebastian.munoz@upc.edu (S. Muñoz-Guerra).

alkyltrimethylammonium bromide salts (*n*ATMA·Br) [8], and it has been conceived with the purpose of evaluating the advantages and disadvantages that derive from the replacement of organoammonium by organophosphonium surfactant concerning the structure and properties of the complexes. Firstly a detailed chemical characterization of *n*ATMP·HyA including their thermal stability was performed. Then the nanostructure adopted by the complexes and their thermal behavior were examined in detail since significant differences between the two complexes series should be expected in these regards from the larger size of the phosphorous atom respect to the nitrogen one. Finally the antimicrobial activity against bacteria, including Gram-negative and Gram-positive species, as well as against a fungus, was evaluated to ascertain to what extent the biocide activity of *n*ATMP surfactants is retained once that ionic complexes are formed.

2. Experimental

2.1. Materials

The sodium salt of hyaluronic acid (Na·HyA) with a weight-average molecular weight of about 50,000 Da used in this work was purchased from Enze Chemicals. Alkyltrimethylphosphonium surfactants (*n*ATMP·Br with *n* values from 12 to 22) were synthetized by a procedure previously described by us [23] based on the reaction between the corresponding 1-bromoalkane and a trimethylphosphine solution in toluene.

2.2. Measurements

FTIR spectra were recorded within the 4000–600 cm^{-1} interval on a FTIR Perkin Elmer Frontier spectrophotometer provided with a universal ATR sampling accessory for the examination of solid samples. ^{1}H NMR spectra were recorded on a Bruker AMX-300 NMR instrument operating at 300.1 MHz and using TMS as internal reference. Deuterated methanol and water were used as solvents. Thermogravimetric analyses (TGA) were performed on a Mettler-Toledo TGA/DSC 1 Star System over the 30 to 600 °C interval at a heating rate of 10 °C·min^{-1} under an inert atmosphere. Sample weights of 10–15 mg were used for TGA analysis. Calorimetric measurements (DSC) were carried out on a Perkin-Elmer DSC 8000 instrument calibrated with indium and zinc. Heating-cooling cycles at a rate of 10 °C·min^{-1} within the −30 to 120 °C temperature range under a nitrogen atmosphere were applied in these assays using sample weights of 2–5 mg. Real time X-ray diffraction studies were performed using X-ray synchrotron radiation at the BL11 beamline (NCD, Non-Crystalline Diffraction) of ALBA synchrotron in Cerdanyola del Vallès, Barcelona. Simultaneous SAXS and WAXS were taken from powder samples subjected to heating-cooling cycles at a rate of 10 °C·min^{-1}. The radiation energy employed corresponded to a 0.10 nm wavelength, and spectra were calibrated with silver behenate (AgBh) and Cr$_2$O$_3$ for SAXS and WAXS, respectively. The nanostructure morphology of *n*ATMP·HyA complexes was visualized using a Philips TECNAI 10 transmission electron microscope operating at 100 kV. Specimens were prepared by casting a solution of *n*ATMP·HyA complexes in MeOH:BuOH (4:1) over a water surface. Pieces of the floating film were picked up with carbon coated grids and stained with phosphotungstic acid (PTA) previous to observation.

2.3. Complexes formation and films preparation

The procedure initially reported by Ponomarenko et al. [24] for the synthesis of complexes of poly(α-amino acids) and ionic surfactants has been used in this work. The Ponomarenko's methodology with some minor modifications has been extensively used in our group for coupling either PGGA (poly-γ-glutamic acid) or polyuronic acids with quaternary ammonium salts bearing long linear alkyl chains [8, 25–27] and also for the preparation of *n*ATMP·PGGA complexes

[28]. The methodology essentially consists of adding dropwise an aqueous solution of the *n*ATMP·Br salt to an aqueous solution of Na·HyA at a temperature between 25 and 65 °C (depending on the water solubility of the surfactant), and keeping the mixture under stirring for several hours. The complex is recovered as a white precipitate, which is isolated by centrifugation, repeatedly washed with water, and finally dried under vacuum for at least 24 h.

Films preparation was carried out by casting a solution of the *n*ATMP·HyA complex in methanol on 3 × 3 cm^2 Petri plates. After drying at room temperature, films were cut as either 1 × 1 cm^2 squares or 5 mm-diameter discs, and further dried under vacuum for 24 h. Film thickness were estimated to be 115 ± 10 μm as measured by a Mitutoyo micrometer (Osaka, Japan).

2.4. Hydrolytic degradation and release of nATMP surfactant

For degradation studies, discs of *n*ATMP·HyA complexes with *n* = 16 and 22 were placed in vials to which 5 mL of the corresponding buffer solution were added. Phosphate buffers pH 7.4, either with or without enzymes added, and pH 5.5 were the solutions used for incubation. Sealed vials were stored at 37 °C in a heat chamber and discs were taken out at scheduled times, washed with distilled water, dried under vacuum at room temperature, and finally weighted. Chemical modifications involved in degradation were followed by NMR analysis of both, the remaining disk and the products released to the degradation medium.

For measuring the amount of *n*ATMP released from complexes upon incubation in aqueous medium, discs were placed into cellulose membrane tubes (2000 Da cut-off) which were then introduced in vials containing 10 mL of buffer solution and subjected to gentle stirring for 24 h. Assays were carried out at pH 7.4 (at 25 and 37 °C) and 5.5 at 25 °C. The amount of released *n*ATMP was determined by measuring the absorbance of the dialysate at 208 nm at scheduled times.

2.5. Antimicrobial activity of complexes

The antimicrobial activity of *n*ATMP·HyA complexes was tested *in vivo* against *Staphylococcus aureus* CECT 6538 and *Escherichia coli* ATCC 9001 as Gram-positive and Gram-negative bacteria, respectively, and against *Candida albicans* CECT 1392 as yeast. All the microorganisms were tested in both solid and liquid culture media following the experimental procedure described by Muriel-Galet et al. [29]. Bacterial cultures were incubated in TSA (Triptic Soy Agar, Difco Laboratories) for 24 h at 37 °C and then transferred to a TSB (Triptic Soy Broth) medium where they were left to grow for 18 h at 37 °C to assess their exponential growth. Cultures were then diluted to obtain the desired concentration which was fixed at 7.2·10^7 and 1.59·10^7 CFU·mL^{-1} (OD$_{600}$ = 0.9, in the solid medium) and at 1.37·10^5 and 4.67·10^5 CFU·mL^{-1} (OD$_{600}$ = 0.2, in the liquid medium) for *S. aureus* and *E. coli*, respectively. *C. albicans* cells were left to grow for 18 h at 30 °C in Potato Dextrose Broth (PDB) medium. Cultures were then diluted to obtain 1.33·10^5 (OD$_{600}$ = 1.06) and 1.26·10^3 (OD$_{600}$ = 0.2) concentration for solid and liquid media, respectively.

The antimicrobial activity on solid media was tested using the agar diffusion method which consists of spreading 100 μL of microorganism solution over a prepared TSA or TSB (for *C. albicans*) surface, and placing the 5 mm-diameter film disk at the center of a Petri dish. Plates were incubated at 37 °C for 24 h and the diameter of the resulting inhibition zone was measured directly after the incubation period. HyA was used as negative control and all measurements were made in triplicate.

The antimicrobial activity in liquid media was tested immersing 1 × 1 cm^2 film squares of *n*ATMP·HyA complexes in 10 mL of TSB (PDB for *C. albicans*) containing 100 μL of each microorganism for incubation at 22 °C during 24 h. For quantification, 100 μL aliquots were removed from the suspension at scheduled times, diluted with peptone buffer solution and plated in triplicate in Petri dishes in a TSA (or PDA for
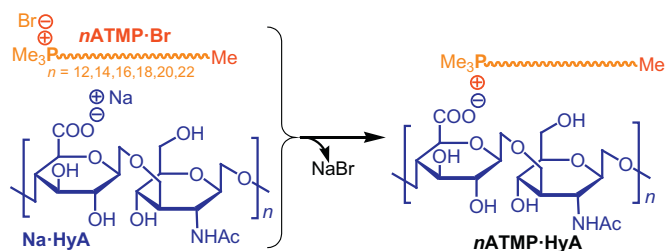
Scheme 1. Coupling reaction of *n*ATMP·Br surfactants with hyaluronic acid (HyA) leading to *n*ATMP·HyA ionic complexes.

C. albicans) culture medium. Colonies were counted after incubation at 37 °C for 24 h in triplicate.

To study the effect of temperature and pH in the antimicrobial activity of *n*ATMP·HyA films, the growth curve of each microorganism was studied alone and in the presence of compounds released from the complexes upon incubation. Colony counting was made by photometric measurement using a Tecan's Magellan™ instrument. Firstly, each film was immersed in tubes containing 10 mL of TSB (or PDB for *C. albicans*) at pH 7.4 at 22 °C for 24 h. Then 100 μL of the supernatant liquid was transferred to ELISA plates containing 100 μL of *S. aureus*, *E. coli* or *C. albicans* and incubated at 37 °C for 24 h under agitation. Measurements were made in triplicate at $\lambda = 490$ nm at regular periods over the whole incubation period.

3. Results and discussion

3.1. Synthesis and chemical characterization of nATMP·HyA complexes

The coupling reaction of *n*ATMP·Br and Na·HyA (Scheme 1) provided the ionic *n*ATMP·HyA complexes with even *n* values from 12 to 22. The solubility displayed by the *n*ATMP·HyA complexes was in agreement with what should be expected for polymers with a strong amphiphilic character, *i.e.* they were soluble in methanol but nonsoluble in either water or chloroform. The reaction conditions used for the synthesis and the results therein obtained are presented in Table 1.

In all cases, equimolar amounts of polyacid and surfactant were mixed at the minimum temperature required to have the alkyltrimethylphosphonium salt fully dissolved in water. Yields ranged between 55 and 90% with values increasing steadily with the length of the surfactant alkyl tail. Yields of complexes with lower values of *n* could not be enhanced despite using higher concentration solutions.

The chemical constitution of the *n*ATMP·HyA complexes was ascertained by both FTIR and NMR spectroscopies. As an example of the information provided by FTIR, the spectrum of 18ATMP·HyA together with those of the sodium salt of hyaluronic acid (Na·HyA) and octadecyltrimethylphosphonium bromide (18ATMP·Br) are represented in Fig. 1a. The spectrum recorded from the complex showed the characteristic bands of hyaluronic acid at 3340 cm^{-1} (O—H and
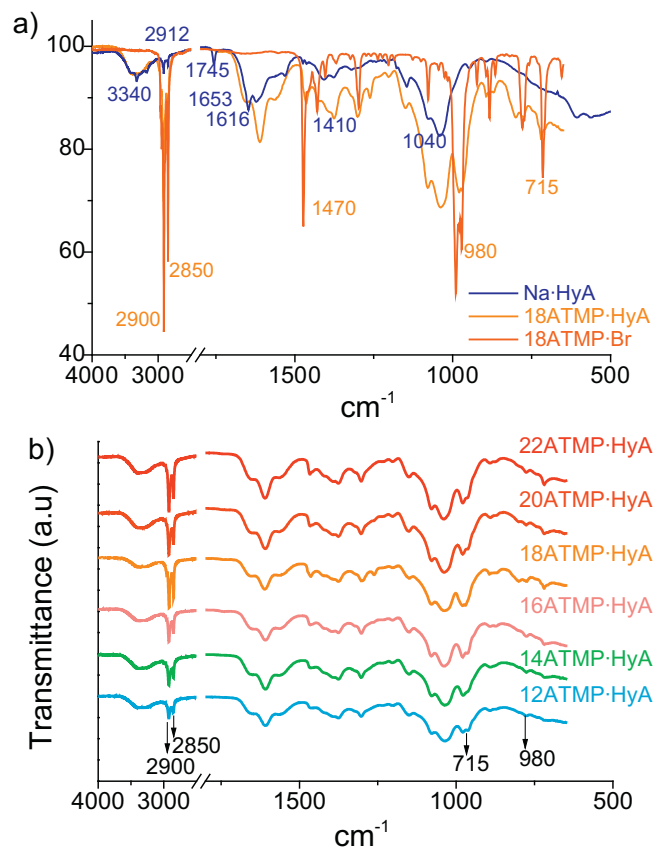

Fig. 1. FTIR recorded at 25 °C from a) 18ATMP·Br, Na·HyA and 18ATMP·HyA complex, and b) the whole series of *n*ATMP·HyA complexes.

N—H stretching), 1616 and 1410 cm^{-1} (asymmetric and symmetric C—O stretching modes of the planar carboxylate group), 1653, 1563 and 1320 cm^{-1} (amide I, II, and III bands, respectively) and 1040 cm^{-1} (C-O-C stretching) [30,31]. Additionally the two bands at 990 and 715 cm^{-1} which are attributable to the P—C stretching vibrations in the alkylphosphonium groups [32,33], were present with strong intensity. The weak band appearing at 1745 cm^{-1} in the spectrum of Na·HyA could be associated to the C=O stretching of a small amount of COOH group present in the sample, which as expected was absent in the spectrum of the complex. The spectra recorded for the whole series of complexes are comparatively represented in Fig. 1b where the close similitude existing among them can be appreciated. The only difference clearly noticed is that concerning the intensity of the C—H stretching bands appearing at ~2900 and ~2850 cm^{-1}, which as expected, increases steadily with the value of *n*. The ^{1}H NMR spectrum recorded from the 18ATMP·HyA complex is reproduced in Fig. 2 and the collection recorded from the whole series may be inspected in Fig. S1.

Table 1
Results for the preparation of *n*ATMP·HyA complexes.

*n*ATMP·HyA	Mixing conditions		Yield	Elemental analysis[c]			Composition[d]
	c (M)[a]	*T* (°C)[b]	(%)	C (%)	H (%)	N (%)	ATMP:HyA:H$_2$O
12ATMP·HyA	0.075	25	55	53.3 (52.8)	8.5 (8.9)	2.0 (2.1)	1.0:1.0:2.0
14ATMP·HyA	0.05	25	65	56.5 (55.6)	9.4 (9.0)	1.9 (2.1)	1.0:1.0:1.0
16ATMP·HyA	0.01	25	70	57.0 (57.3)	9.6 (9.3)	1.8 (1.9)	1.0:1.0:0.75
18ATMP·HyA	0.01	45	75	58.6 (58.6)	10.1 (9.4)	1.7 (1.9)	1.0:1.0:0.5
20ATMP·HyA	0.01	55	85	59.6 (59.7)	10.2 (9.7)	1.6 (1.8)	1.05:1.0:0.5
22ATMP·HyA	0.01	65	90	60.7 (60.8)	10.5 (9.9)	1.5 (1.7)	1.1:1.0:0.5

[a] Molar concentration of the two solutions mixed to form the complex.
[b] Mixing temperature selected according to the surfactant solubility in water.
[c] Experimental content percentages of C, H and N. The calculated values are indicated in parenthesis.
[d] Ratio of ATMP to HyA and to H$_2$O in the complex consistent with elemental analysis.
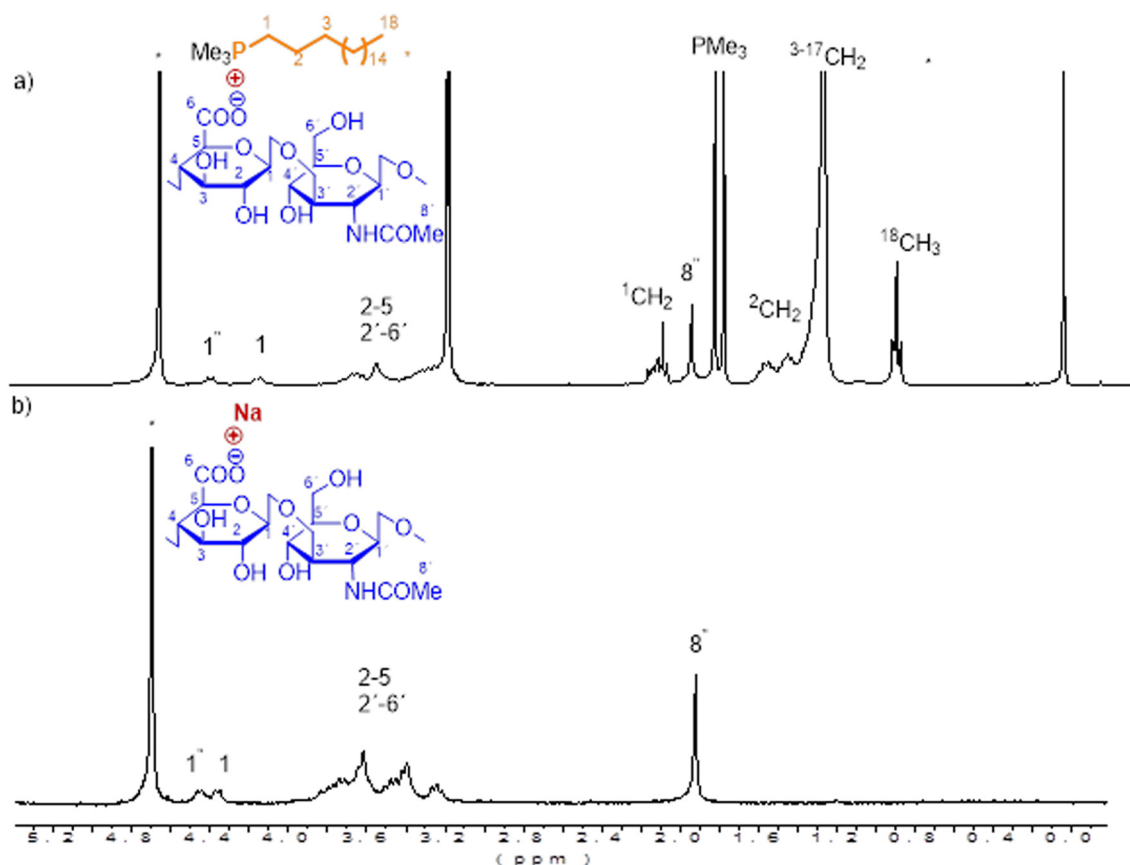
Fig. 2. ^{1}H NMR spectra of 18ATMP·HyA complex in MeOD (a) and hyaluronic acid in D$_2$O (b) recorded at 25 °C. *Residual protons of deuterated solvents.

In these spectra, all the signals arising from both the polyacid and surfactant counterparts could be properly assigned to the chemical structure expected for the complexes. However, signal overlapping and broadening, the latter probably due to the restricted mobility of the HyA chain, prevented determining with reliability the complex composition by signal area quantification.

Nevertheless an approximate evaluation of the composition of the complexes could be made on the basis of the atomic composition provided by the combustion analysis data by assuming that a certain amount of water is adsorbed in the complex. The resulting values are given in Table 1 and a graphical representation of the reasonably acceptable compositional domain in terms of surfactant/hyaluronic acid ratio and adsorbed water is depicted in Fig. S2. These calculations revealed that the nATMP:HyA ratio in nATMP·HyA complexes may oscillated between 1.0 and 1.1 with values slightly increasing with the length of the alkyl side chain. The amount of water present in these complexes would range between 0.5 and 2 mol per mole of HyA, as it was inferred by

fitting experimental and calculated atom percentages in the elemental analysis. As expected, the longer is the alkyl chain the lower is the amount of water that is adsorbed in the complex.

3.2. Thermal properties of nATMP·HyA complexes

The thermal stability of nATMP·HyA complexes under an inert atmosphere was examined by TGA. The most significant thermogravimetric parameters are collected in Table 2 and the recorded traces for the whole series together with their corresponding derivative curves are shown in Fig. 3. All traces presented in Fig. 3a show a slight weight loss at temperatures around 100 °C which is interpreted as due to the release of adsorbed water. Thermal onset decomposition temperatures are between 200 and 210 °C which is the range in which HyA starts to decompose (Fig. S3) but they are much lower than the ^oT_d reported for nATMP·Br surfactants [23, 34]. Apparently the thermal stability of HyA is not improved by the presence of the organophosphonium

Table 2
Thermal parameters of nATMP·HyA complexes.

Complex	TGA[a]			DSC[b]								
				1st heating			Cooling			2nd heating		
	^oT_d (°C)	$^{max}T_d$ (°C)	W (%)	T_m (°C)	ΔH_m (Kcal·mol^{-1})	n_c	T_m (°C)	ΔH_m (Kcal·mol^{-1})	n_c	T_m (°C)	ΔH_m (Kcal·mol^{-1})	n_c
12ATMP·HyA	207	219/306/430	12	–	–	–				–	–	–
14ATMP·HyA	205	219/312/432	11	–	–	–				–	–	–
16ATMP·HyA	200	219/330/437	9	–	–	–				–	–	–
18ATMP·HyA	209	219/340/437	10	58	1.9	2	43	1.2		48	1.1	1
20ATMP·HyA	203	216/350/437	11	67	3.1	4	62	1.4		64	2.1	3
22ATMP·HyA	205	216/350/437	7	70	5.2	6	65	3.7		69	4.5	5

[a] ^oT_d and $^{max}T_d$: onset and maximum rate decomposition temperatures; W: remaining weight at 600 °C.
[b] DSC traces recorded in the −20–80 °C interval; T_m: melting temperature; ΔH_m: melting enthalpy; n_c: calculated number of crystallized methylenes in the alkyl chain.
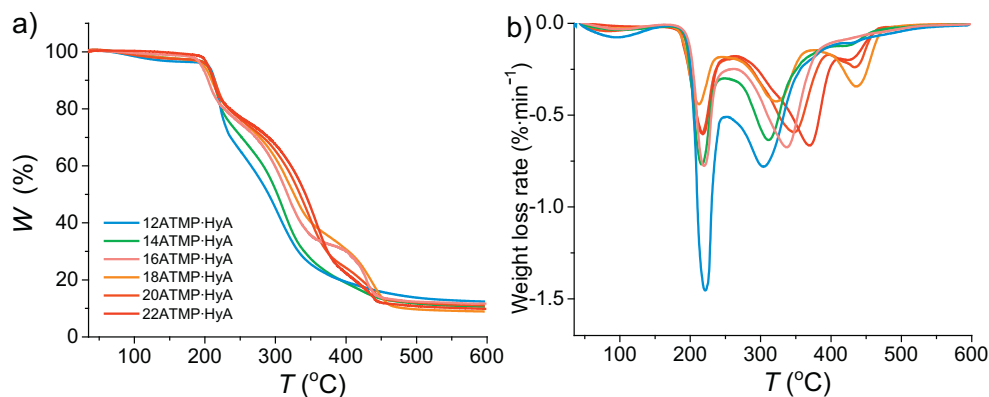
Fig. 3. TGA traces of nATMP·HyA complexes (a) and their derivative curves (b).

counterpart, which is a result contrary to that reported for complexes made of poly(γ-glutamic acid) coupled with the same surfactants [28].

The derivative curves shown in Fig. 3b clearly revealed that thermal decomposition proceeded in all cases trough a multi-stage process involving at least three stages with maximum loss weight rates at temperatures in the 215–220 °C, 300–350 °C and 430–440 °C ranges, respectively, to leave <10% of the initial mass at the end of the whole process. The $^{max}T_d$ for the first stage appeared fairly constant along the whole series of complexes indicating that decomposition of the hyaluronic acid must be the main process taking place at this stage. Conversely, the second and third maximum decomposition temperatures increased steadily with n, suggesting that decomposition of the surfactant should be involved in the two last stages. The molecular mechanism of the thermal degradation of the nATMA·PGGA complexes has been studied in detail and reported to proceed through two stages, the former taking place at temperatures increasing with n and involving the simultaneous decomposition of the complex and the polyacid [35]. On the other hand, nATMA·HyA complexes have been reported to decompose through a multi-stage process with the $^{max}T_d$ for the first stage being almost constant at a value within the 215–225 °C range [8]. Unfortunately the thermal decomposition of neither HyA nor their derivatives has been studied in detail and the information accessible on this topic is scarce [36,37]. At this moment, little more can be said about the mechanism operating in the thermal decomposition of nATMP·HyA complexes.

The DSC study was performed by subjecting the nATMP·HyA samples to heating-cooling cycles over the −30–120 °C range. As it is

shown in Fig. 4a, only heating traces of complexes with $n \geq 18$ showed endothermic peaks, which appear at temperatures steadily increasing from 55 °C up to 70 °C. According to what is well known for other related ionic complexes [25–28], such endothermic peaks must be associated to the melting of the paraffinic phase made of crystallized alkyl chains. Comparison of these results with those reported for nATMP·PGGA complexes, in which crystallinity could be observed for $n \geq 16$ [28], led to infer that, compared to PGGA, HyA is more effective in disturbing the lateral arrangement required by the alkyl chains to crystallize.

Recrystallization of nATMP·HyA from the melt was highly depending on the temperature at which the sample was previously heated. Fig. 4b shows that no crystallization occurred in 18ATMP·HyA upon cooling from 120 °C whereas melting peaks could be partially recovered when the first heating was limited to 80 °C. Similar results were obtained for 20ATMP·HyA and 22ATMP·HyA complexes (Fig. S4). Such a different behavior is doubtlessly a consequence of the nucleating effect that is able to operate in samples subjected to moderate overheating. Melting temperatures and enthalpies measured for the recrystallized samples are given in Table 2.

The graphical representation of ΔH_m against n (Fig. 5) revealed an almost linear dependence between these two variables. The equation resulting from these data provides the individual methylene (ΔH_m^{CH2}) and non-methylene (ΔH_m^0) contributions to the experimentally observed melting enthalpy as the slope and the y-axis intercept at $n = 0$, respectively [38, 39]. The average amount of crystallized methylene units per alkyl chain is given by $n_c = K + n$, where n_c is the minimum
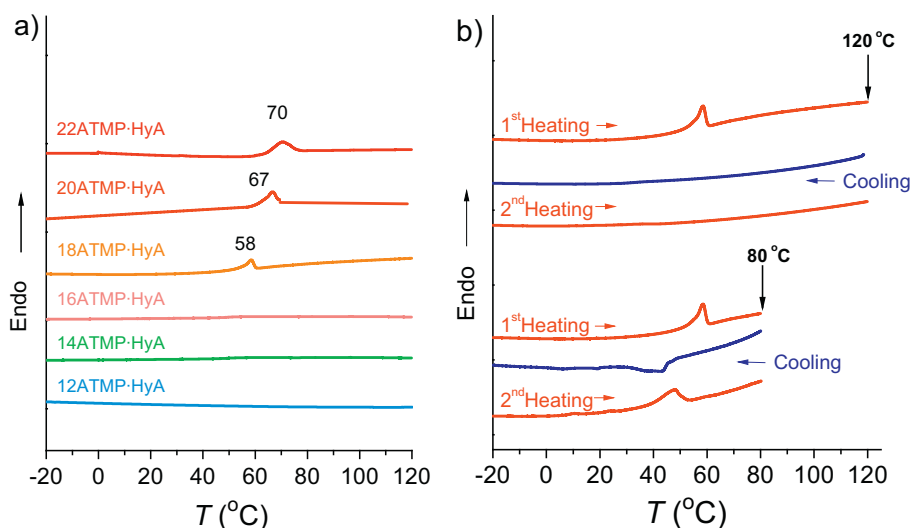

Fig. 4. a) First heating DSC traces of nATMP·HyA complexes. b) DSC traces of 18ATMP·HyA complex recording at heating and cooling within the −20–120 °C and −20–80 °C intervals.
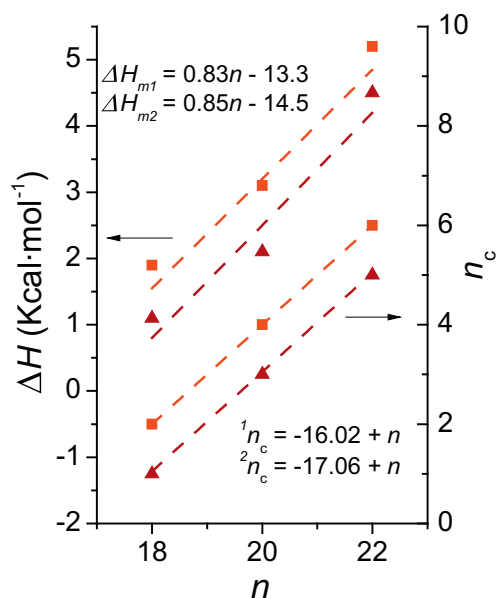
$\Delta H_{m1} = 0.83n - 13.3$
$\Delta H_{m2} = 0.85n - 14.5$

$^{1}n_c = -16.02 + n$
$^{2}n_c = -17.06 + n$

Fig. 5. Plots of melting enthalpy (ΔH_m) and number of crystallized methylenes (n_c) for 18, 20 and 22ATMP·HyA complexes against the number of carbons contained in the alkyl side chain. Squares and triangles refer to values obtained in the first heating and the second heating of samples crystallized from samples previously heated at 80 °C.

number needed for crystallization. As it is represented in Fig. 5 and given in Table 2, n_c oscillates between 1 and 6 depending on chain length and thermal history. These values are much lower than those reported for nATMP·PGGA complexes [28] but comparable to those reported for nATMA·HyA [8], a result that confirms the influence of the polymer chain on the crystallizability of the attached surfactant.

3.3. Structure of nATMP·HyA complexes. Temperature effects

To gather information on both the supramolecular structure and the packing of the alkyl side chains in nATMP·HyA, as well as to evaluate the effect of heating on the structure, these complexes were examined at real time by X-ray diffraction at variable temperature. Wide and small angle scattering (WAXS and SAXS, respectively) were simultaneously recorded from samples subjected to heating or cooling over the 10–120 °C interval.

3.3.1. XRD and TEM analysis at room temperature

The SAXS and WAXS profiles recorded at 25 °C from the whole series are compared in Fig. 6, and the spacings measured at different temperatures are collected in Table 3. The scattering produced in the SAXS region by all the complexes (Fig. 6a) consisted of three main peaks with spacings between 3 and 5 nm and variable intensity. According to a number of studies carried out on similar comb-like amphiphilic systems [8,25–28], this scattering is interpreted to arise from the periodicity of the biphasic nanostructure in which the complexes become self-assembled. In previously examined cases, a stratified structure with the polyelectrolyte and the paraffinic moiety of the surfactant separated in two phases that alternate regularly with an interlayer spacing that increases monotonically with the length of the alkyl chain, was commonly described.

In the present case however the occurrence of multiple scattering is indicative of a more complex structure. Interestingly, an approximate ratio of 1:1.1:1.2 is assessed for the spacings associated to the three peaks seen in SAXS indicating that a close structural interrelation must exists among them. Furthermore, linear correlations are detected for the spacings of complexes with $n \leq 16$ and for the complexes with $n \geq 18$. A mixture of different arrangements all them fitting in a common structural pattern may be in principle consistent with SAXS results. On the other hand, the scattering exhibited in the WAXS region (Fig. 6b) for all the complexes consisted of a broad scattering centered on ~0.45 nm, which is known to be characteristic of a disordered packing of the polymethylene chains. In addition 18ATMP·HyA, 20ATMP·HyA and 22ATMP·HyA showed a shoulder at ~0.41 nm that is associated to the pseudo hexagonal lattice commonly adopted by the paraffinic phase in this type of complexes [25,26].

The TEM examination of films of these complexes prepared by casting on a water surface provided useful information that greatly helped the interpretation of X-rays diffraction results. Representative micrographs recorded from films of 16ATMP·HyA and 22ATMP·HyA are shown in Fig. 7. In both cases, a banded texture of alternating clear and dark stripes with an average periodicity oscillating between 3 and 6 nm was clearly observed in good agreement with the spacings observed by SAXS. It is worthy noticing the waving appearance observed in the case of 16ATMP·HyA, which is reminiscent of the typical fingerprint texture displayed by soft phospholipid membranes. On the contrary, the essentially straight traces observed for 22ATMP·HyA indicate the presence of a much stiffer structure in this complex. The observed differences are thought to be motivated by the different state of the paraffinic phase in each case, i.e. crystallized for $n = 22$ but uncrystallised for $n = 16$. In addition to the banded texture, nanometric round
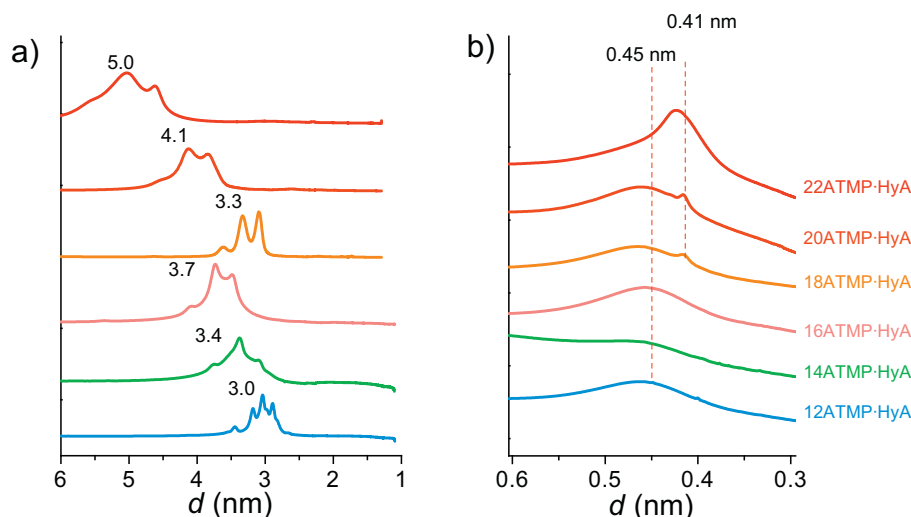

Fig. 6. XRD profiles recorded at room temperature from nATMP·HyA in the SAXS (a) and WAXS regions (b).

Table 3
X-ray diffraction data of nATMP·HyA complexes.

Complex	SAXS[a]			WAXS		
	$L_0^{10°C}$	$L_0^{120°C}$	$L_0^{10°C}$	$d_{100}^{10°C}$	$d_{100}^{120°C}$	$d_{100}^{10°C}$
12ATMP·HyA	3.45, **3.15**, 2.90	3.44, 3.18, 2.88	3.39, 3.12, 2.84	0.45	0.45	0.45
14ATMP·HyA	3.75, **3.40**, 3.10	3.79, 3.39, 3.12	3.68, 3.35, 3.08	0.45	0.45	0.45
16ATMP·HyA	4.06, **3.71**, 3.38	4.35, 3.91, 3.44	4.37, 3.89, 3.42	0.45	0.45	0.45
18ATMP·HyA	3.66, **3.36**, 3.05	3.76, 3.44, 3.76	3.78, 3.43, 3.77	0.41	0.45	0.45
20ATMP·HyA	4.57, **4.14**, 3.82	4.55, 4.18, 3.96	4.45, 4.13, 3.86	0.41	0.45	0.45
22ATMP·HyA	5.52, **5.06**, 4.60	5.61, 5.07, 4.67	5.48, 4.98, 4.49	0.41	0.45	0.45

[a] Main peaks in bold.

particles more or less hexagonally packed are frequently seen on these pictures, more ostensibly in the case of 16ATMP·HyA. The optical diffraction analysis of selected areas allowed an approximate determination of the periodical spacings present in these complexes (Figs. S5 and S6), which were consistent with those measured by SAXS. Biphasic lamellae, cylinders and spheres are possible nano-arrangements compatible with the pictures obtained by TEM. Further efforts addressed to identify without ambiguity the different observed morphologies and to relate them with the information provided by XRD are needed to achieve an accurate description of the nanostructure of these complexes.

3.3.2. Temperature effects on the structure of nATMP·HyA complexes

The effect of temperature on the structure of nATMP·HyA complexes was examined by XRD at real time using synchrotron radiation. Samples were subjected to heating-cooling cycles from 10 °C to 120 °C at a heating/cooling rate of 10 °C·min^{-1}. Spacings observed at the beginning and the end of each run for the whole series of complexes is compared in Table 3. The detailed changes taking place on the X-ray diffraction profiles of 16ATMP·HyA and 22ATMP·HyA, with temperature in both SAXS and WAXS regions, are shown in Figs. 8 & 9, respectively. Similar graphical representations for all the other complexes are included in Figs. S7–S10 of the SM file.

The general behavior observed in the SAXS profiles (Fig. 8) consists of a slight change in the L_0 spacing with temperature that does not follows any recognizable trend along the series for none of the observed peaks. This result strongly contrasts with those observed for analog complexes made from PGGA where a clear L_0 changing effect was shared by the whole series upon heating or cooling. On the contrary, significant differences were observed in WAXS profiles for the two series and also among the members of the same series. WAXS profiles of complexes with $n \leq 16$ hardly changed with temperature so that the initial profile observed at 10 °C was maintained invariable along the whole heating-cooling cycle (Fig. 9a and a′). Conversely, WAXS profiles of complexes with $n \geq 18$ were sensitive to heating with the 0.41 nm peak characteristic of the crystallized paraffinic phase disappearing at
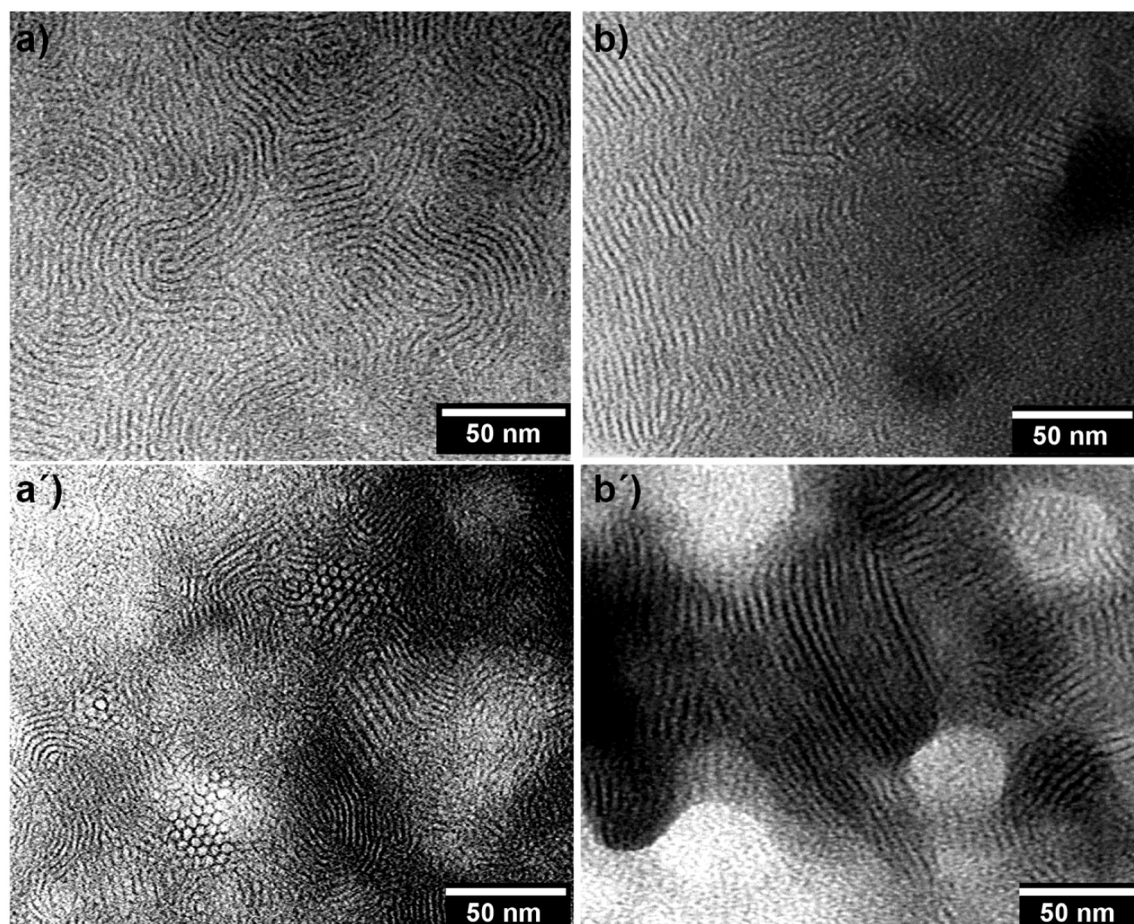

Fig. 7. TEM micrographs of 16ATMP·HyA (a and a′) and 22ATMP·HyA (b and b′) films obtained by casting.
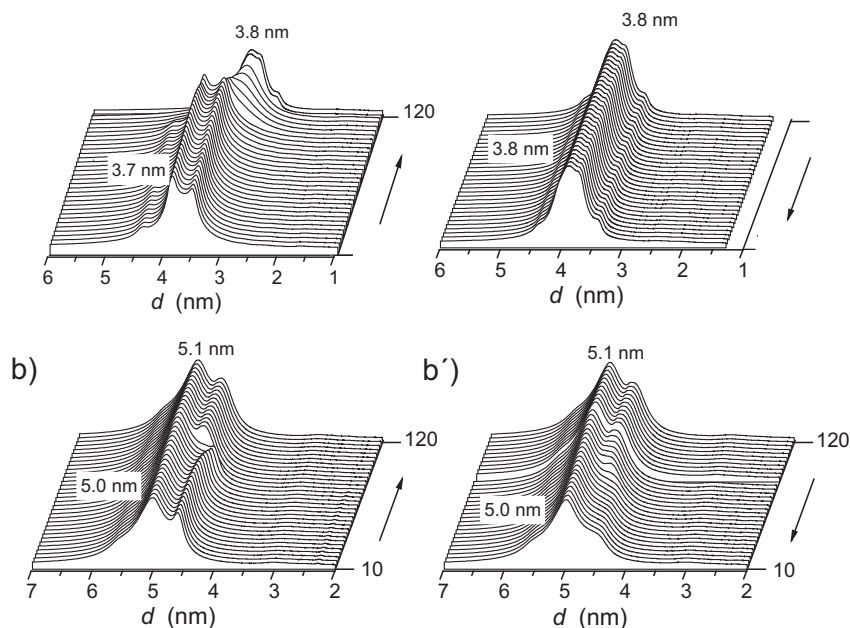
Fig. 8. SAXS and WAXS profiles of 16ATMP·HyA and 22ATMP·HyA at heating (a and b) and cooling (a′ and b′) along 10–120 °C range.

the melting temperature. At 120 °C the broad peak at 0.45 nm characteristic of a disordered phase was the only one observed for all complexes (Fig. 9b). After cooling, the peak at 0.41 nm was barely recovered (Fig. 9b′) revealing the poor crystallizability of these complexes.

To appraise more accurately the reversibility of the melting-cooling process of nATMP·HyA complexes with $n \geq 18$, XRD of 22ATMP·HyA was registered from samples subjected to a heating-cooling cycle over the 10–80 °C range. The changes seen in SAXS were similar to that observed when samples were heated to 120 °C whereas WAXS profiles revealed that the complex was able to crystallize upon cooling (Fig. S11). These results give support to those obtained by DSC previously described, and confirm the critical importance of the self-nucleating process on the ability of the surfactant alkyl chain to crystallize in these complexes.

3.4. Decomposition of nATMP·HyA complexes in aqueous environment

The changes in sample weight of two nATMP·HyA complexes differing in n, *i.e.* 16ATMP·HyA and 22ATMP·HyA, that take place upon incubation in an aqueous environment were comparatively examined under different conditions in order to evaluate the effect of the length of the alkyl chain, pH and enzymes on the susceptibility of complexes to water attack. Both dissociation of the ionic pair and hydrolysis of the polysaccharide chain are expected to occur in more or less extent by the action of water. The weight losses taking place at pH 5.5 and 7.4, in the latter case with or without enzymes added, are plotted in Fig. 10a. The results clearly revealed that the complexes with $n = 16$ decomposed faster than those with $n = 22$ at both pHs. This is more than reasonable since the paraffinic moiety of the surfactant is expected
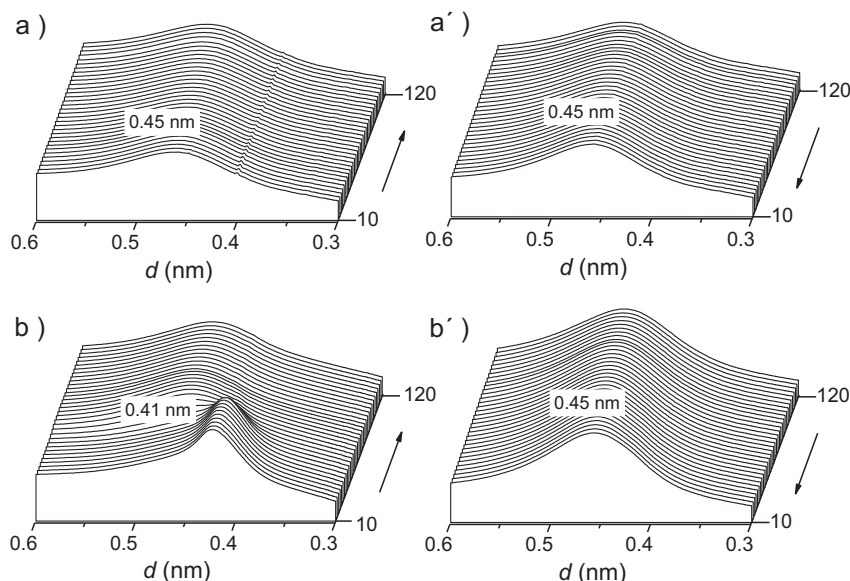

Fig. 9. SAXS and WAXS profiles of 16ATMP·HyA and 22ATMP·HyA at heating (a and b) and cooling (a′ and b′) along 10–120 °C range.
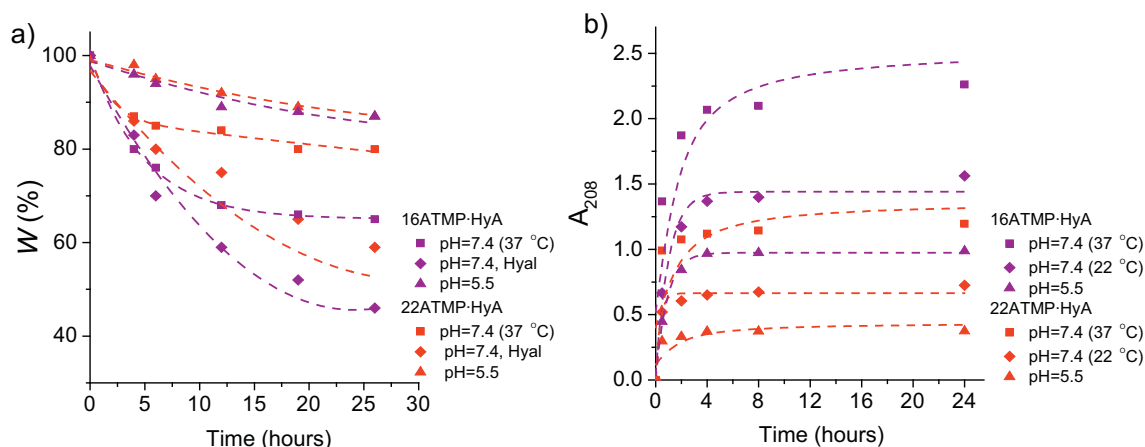
Fig. 10. a) Weight loss undergone by *n*ATMP·HyA complexes with *n* = 16 and 22 upon incubation at 37 °C at different pHs and either with or without enzymes (Hyal) added. b) Release of the *n*ATMP for *n* = 16 and 22 from their respective *n*ATMP·HyA complexes under the indicated conditions.

to hinder the access of water to the polymer main chain. It was also shown that decomposition proceeded at much higher rates at physiological pH than at acidic pH for the two complexes. In fact, both complexes lost only 10% of their initial weight at pH = 5.5 along the whole incubation period whereas at pH = 7.4 the lost weight was near 40% and 20% for 16ATMP·HyA and 22ATMP·HyA, respectively. The action of enzymes was really noticeable since weight losses arrived to be >50% when the complexes were incubated in the presence of hyaluronidases (Hyal). This result is remarkable since it demonstrated that HyA continues being sensitive to enzymes after being ionically coupled with organophosphonium compounds [40].

The release of ATMP from *n*ATMP·HyA complexes was studied as a prediction of their biocide activity. Although the capability of HyA to repress the growth of certain microorganisms has been claimed by different authors, the biocide activity of the complexes is expected to be essentially determined by the organophosphonium counterpart. The more surfactant is released to the aqueous environment, the higher should be the antimicrobial activity displayed by the *n*ATMP·HyA complexes. ATMP is released from the complexes as a consequence of the dissociation undergone by the ionic pair, and the releasing rate will depend on the water solubility of both trimethylalkylphosphonium cation and HyA as well as on incubation conditions. The dissociation of complexes in water with concomitant release of the surfactant was estimated by measuring the increase of absorbance at 208 nm of the incubation medium as a function of time for a total period of 24 h at either 22 °C (pH 5.5 and 7.4) or 37 °C (pH 7.4). The results are plotted in Fig. 10b where it is clearly seen how the dissociation equilibrium was reached after 4–6 h of incubation. A simple comparison of the resulting curves brings into evidence also that 16ATMP was released faster than 22ATMP whichever were the conditions used. This is quite reasonable given the relative solubility in water of the two surfactants. Regarding pH and temperature, maximum dissociation was found to happen at pH 7.4 at 37 °C. Whereas the favourable effect of temperature on release rate does not need supporting explanation, the greater dissociation observed at neutral conditions for the two complexes should be related to the effect that pH has on the solubility of the surfactant.

NMR analysis provided valuable information in support of the results obtained from weight loss and absorbance measurements (Fig. S12). The ^{1}H NMR spectra of discs residues remaining after incubation showed scarce differences with those recorded from the initial ones. It does mean that no significant chemical changes other than hydrolysis of HyA took place upon incubation. The observed weight loss must correspond therefore to the release of *n*ATMP·HyA short fragments generated by hydrolysis of the polysaccharide chain with enough low molecular weight as to be water-soluble. This is in agreement with what was seen on the spectra recorded from the releasing medium

which showed surfactant signals only when enzymes were used for degradation.

3.5. Antimicrobial activity of nATMP·HyA complexes

The antimicrobial activity of films of *n*ATMP·HyA complexes was evaluated against bacteria *S. aureus* (Gram-positive) and *E. coli* (Gram-negative) and against the common yeast *C. albicans* by using both solid and liquid media methodologies. 16ATMP·HyA and 22ATMP·HyA complexes were selected for this study.

Results obtained with the solid-medium method using agar as substrate are gathered in Table 4 where the diameter of the inhibition area observed for every microorganism is compared for the two complexes and for uncoupled HyA. No inhibition area was observed at any case when culture was performed on HyA which is taken as indicative of the inactivity of this compound against the tested microorganisms. On the contrary, a considerable growth inhibiting capacity against bacteria was displayed by both 16ATMP·HyA and 22ATMP·HyA, which was found stronger for the former when *S. aureus* was the microorganism assayed. This result is very according to expectations since the high biocide effectivity of cationic surfactants against Gram-positive bacteria is a well-known fact [41]. The results obtained for *C. albicans* revealed a poor activity of 16ATMP·HyA against this fungi, which arrived to be inappreciable for 22ATMP·HyA.

Results obtained from biocide assays using liquid media are compared in Fig. 11, and pictures showing the appearance displayed by the incubation medium along the different assays are provided in Fig. S13. The representation of Log(CFU) (Colonia Forming Units) at scheduled incubation times for 16ATMP·HyA and 22ATMP·HyA and their respective surfactants as well as for HyA provides a clear assessment of the biocide capacity of the complexes. Values of Log(CFU) measured at different times for the different assayed systems are collected in Table S1 together with the Log(RV) (Reduction Value) and PR (Percentage of Reduction) values calculated therefrom. In agreement with results afforded by solid media assays, the highest antibacterial activity was displayed by 16ATMP·HyA against *S. aureus* with a total growth

Table 4
Antimicrobial activity of *n*ATMP·HyA films against bacteria and fungi.[a]

Microorganism	HyA	16ATMP·HyA	22ATMP·HyA
S. aureus	0 ± 0.0	29.5 ± 0.9	11.9 ± 0.5
E. coli	0 ± 0.0	15.1 ± 0.3	11.0 ± 0.9
C. albicans	0 ± 0.0	8.3 ± 0.2	0 ± 0.0

[a] Evaluated on a solid medium at 37 °C for 24 h. Zones of growth inhibition (mm) showing antimicrobial activity; film size 5 mm, plate diameter 90 mm. Values for zone of growth inhibition are presented as mean ± SD for triplicates.
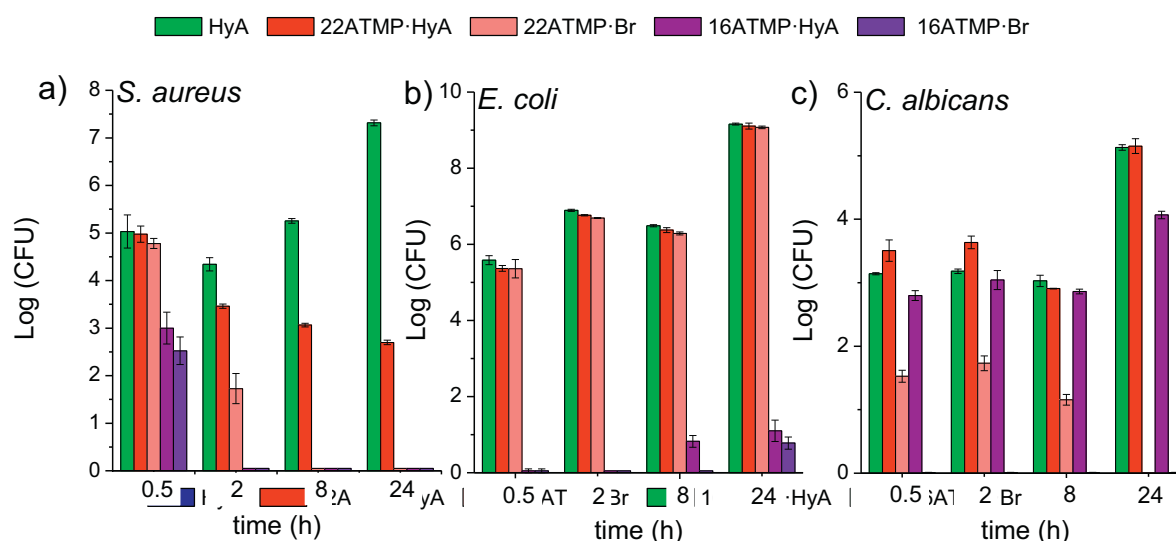
Fig. 11. Antimicrobial activity of 16ATMP·Br, 22ATMP·Br and their complexes with HyA in liquid media against *S. aureus* (a), *E. coli* (b) and *C. albicans* (c).

inhibition after only 2 h of contact. An even faster activity was shown by this complex against *E. coli* reaching an almost total inhibition after 30 min. The behaviour displayed by 22ATMP·HyA was significantly different. The inhibition capacity of this complex against *S. aureus* was also very strong showing a PR of 99.998% after 24 h but its efficiency against *E. coli* was poor with a PR of only 11% after 24 h. Regarding the antifungal activity, results obtained against *C. albicans* revealed a remarkable inhibitory capacity for 16ATMP·HyA that dramatically decreased for 22ATMP·HyA. The antimicrobial activity of HyA for both bacteria and fungi was practically inappreciable whereas surfactants, in particular 16ATMP·Br, exhibited the almost opposite behaviour. A total or nearly total growth inhibition of *S. aureus* and *C. albicans* was attained by the action of both surfactants whereas only 16ATMP·Br displayed strong activity against *E. coli.*

In order to ascertain that the activity displayed by the complexes mainly arose from the compounds that were released to the incubation medium, the growth of microorganisms in the supernatants used for incubating HyA and the complexes films was examined (optical density *vs.* time curves obtained in this study are depicted in Fig. S14). The curves resulting for HyA acid displayed the typical growth evolution profile consisting of lag, exponential and stationary phases. Curves obtained for the supernatants of 16ATMP·HyA and 22ATMP·HyA films were much flatter, in particular for the former complex, bringing into evidence the biocide effect of the dissolved species.

4. Conclusions

Almost stoichiometric *n*ATMP·HyA complexes have been successfully produced by ionic coupling of hyaluronic acid (HyA) with alkyltrimethylphosphonium bromide soaps (*n*ATMP·Br, *n* = 12–22). The structure and thermal properties of these complexes have been examined as a function of *n* and compared with data reported for their analogous complexes made from poly(γ-glutamic acid) (*n*ATMP·PGGA). As their analogues, *n*ATMP·HyA complexes are non-water soluble and also adopt a nanoscopic biphasic arrangement in the solid state. However noticeable differences have been found between the two series as a consequence of the replacement of the polypeptide by the polysaccharide as the polyanionic counterpart of the complex. The thermal stability of *n*ATMP·HyA, although high, is about 100 °C lower than that of *n*ATMP·PGGA, most probably due to the intrinsic low resistance to heat of HyA. Also the crystallizability of the HyA derived complexes is poorer than that of the PGGA derived ones as it is reflected in the lower fraction of methylene units that are able to crystallize and in the higher difficulty found to crystallize from the melt. The greater disturbing effect of HyA on

crystallization is readily understandable taking into account its bulkiness and high interactive capacity by hydrogen bonding. Contrary to what happens in *n*ATMP·PGGA, self-assembling of *n*ATMP·HyA takes place in a much more complex way with generation of more than one biphasic nanostructure that differ among them in the reciprocal arrangement adopted by the surfactant and the biopolymer phases. The response of the *n*ATMP·HyA structure to heating effect is insignificant at the nanoscale level whereas a slight contraction was invariably observed for *n*ATMP·PGGA. Both series of complexes decomposed by the action of water with a similar response to pH changes but the complexes made of HyA showed an extensive degradation in the presence of enzymes. The bactericide activity shown by the two series is similar with a higher intensity when Gram-positive bacteria are concerned. *n*ATMP·HyA complexes display also fungicide activity, a property that was not evaluated for the complexes made of PGGA. In both cases, the biocide activity was found to arise from the organo-phosphonium compounds that are released to water upon incubation. As compared to *n*ATMP·PGGA complexes, differences in either structure or properties including the biocide activity are not significant. Both types of complexes of them are therefore acceptable options for the design of biocompatible/biodegradable antimicrobial films, the preference for one or another being dictated by other properties, such as mechanical or barrier properties and stability in humid environments. These complementary aspects should be assessed in future studies.

Appendix A. Supplementary data

Supplementary data to this article can be found online at https://doi.org/10.1016/j.ijbiomac.2018.07.077.

References

[1] Y. Luo, K.R. Kirker, G.D. Prestwich, Cross-linked hyaluronic acid hydrogel films: new biomaterials for drug delivery, J. Control. Release 69 (2000) 169–184.

[2] J. Baier Leach, K.A. Bivens, C.W. Patrick, C.E. Schmidt, Photocrosslinked hyaluronic acid hydrogels: natural, biodegradable tissue engineering scaffolds, Biotechnol. Bioeng. 82 (2003) 578–589.

[3] J.R. Vazquez, B. Short, A.H. Findlow, B.P. Nixon, A.J.M. Boulton, D.G. Armstrong, Outcomes of hyaluronan therapy in diabetic foot wounds, Diabetes Res. Clin. Pract. 59 (2003) 123–127.

[4] F. Gao, C.X. Yang, W. Mo, Y.W. Liu, Y.Q. He, Hyaluronan oligosaccharides are potential stimulators to angiogenesis via RHAMM mediated signal pathway in wound healing, Clin. Investig. Med. 31 (2008) 106–116.

[5] A. Balazs, E. Leshchiner, Cross-linked gels of hyaluronic acid and products containing such gels, Patent US4582865A, 1987.

[6] J.W. Kuo, D.A. Swann, G.D. Prestwich, Chemical modification of hyaluronic acid by carbodiimides, Bioconjug. Chem. 2 (1991) 232–241.

[7] M. Antonietti, J. Conrad, A. Thuenemann, Polyelectrolyte-surfactant complexes: a new type of solid mesomorphous material, Macromolecules 27 (1994) 6007–6011.

[8] A. Tolentino, A. Alla, A. Martínez De Ilarduya, S. Muñoz-Guerra, Comb-like ionic complexes of hyaluronic acid with alkyltrimethylammonium surfactants, Carbohydr. Polym. 92 (2013) 691–696.

[9] W.J. Macknight, E.A. Ponomarenko, D.A. Tirrel, Self-assembled polyelectrolyte-surfactant complexes in non-aqueous solvents and in the solid state, Acc. Chem. Res. 31 (1998) 781–788.

[10] A. Muñoz-Bonilla, M. Fernández-García, The roadmap of antimicrobial polymeric materials in macromolecular nanotechnology, Eur. Polym. J. 65 (2015) 46–62.

[11] A. Ardizzoni, R.G. Neglia, M.C. Baschieri, C. Cermelli, M. Caratozzolo, E. Righi, B. Palmieri, E. Blasi, Influence of hyaluronic acid on bacterial and fungal species, including clinically relevant opportunistic pathogens, J. Mater. Sci. Mater. Med. 22 (2011) 2329–2338.

[12] P. Pirnazar, L. Wolinsky, S. Nachnani, S. Haake, A. Pilloni, G.W. Bernard, Bacteriostatic effects of hyaluronic acid, J. Periodontol. 70 (1999) 370–374.

[13] M.M. Kemp, A. Kumar, D. Clement, P. Ajayan, S. Mousa, R.J. Linhardt, Hyaluronan- and heparin-reduced silver nanoparticles with antimicrobial properties, Nanomedicine 4 (2009) 421–429.

[14] G. Baier, A. Cavallaro, K. Vasilev, V. Mailänder, A. Musyanovych, K. Landfester, Enzyme responsive hyaluronic acid nanocapsules containing polyhexanide and their exposure to bacteria to prevent infection, Biomacromolecules 14 (2013) 1103–1112.

[15] I. Lequeux, E. Ducasse, T. Jouenne, P. Thebault, Addition of antimicrobial properties to hyaluronic acid by grafting of antimicrobial peptide, Eur. Polym. J. 51 (2014) 182–190.

[16] A. Muñoz-Bonilla, M. Fernández-García, Polymeric materials with antimicrobial activity, Prog. Polym. Sci. 37 (2012) 281–339.

[17] A. Kanazawa, T. Ikeda, T. Endo, Synthesis and antimicrobial activity of dimethyl- and trimethyl-substituted phosphonium salts with alkyl chains of various lengths, Antimicrob. Agents Chemother. 38 (1994) 945–952.

[18] A. Kanazawa, T. Ikeda, T. Endo, Novel polycationic biocides. Synthesis and antibacterial activity of polymeric phosphonium salts, J. Polym. Sci. Part A Polym. Chem. 31 (1993) 335–343.

[19] Y. Xue, H. Xiao, Y. Zhang, Antimicrobial polymeric materials with quaternary ammonium and phosphonium salts, Int. J. Mol. Sci. 16 (2015) 3626–3655.

[20] A. Popa, M. Crisan, A. Visa, G. Ilia, Effect of a phosphonium salt grafted on polymers on cucumber germination and initial growth, Braz. Arch. Biol. Technol. 54 (2011) 107–112.

[21] T. Qiu, Q. Zeng, N. Ao, Preparation and characterization of chlorinated nature rubber (CNR) based polymeric quaternary phosphonium salt bactericide, Mater. Lett. 122 (2014) 13–16.

[22] W. Xie, R. Xie, W.P. Pan, D. Hunter, B. Koene, L.S. Tan, R. Vaia, Thermal stability of quaternary phosphonium modified montmorillonites, Chem. Mater. 14 (2002) 4837–4845.

[23] A. Gamarra, L. Urpí, A. Martínez De Ilarduya, S. Muñoz-Guerra, Crystalline structure and thermotropic behavior of alkyltrimethylphosphonium amphiphiles, Phys. Chem. Chem. Phys. 19 (2017) 4370–4382.

[24] E.A. Ponomarenko, Alan J. Waddon, David A. Tirrell, W.J. MacKnight, Structure and properties of stoichiometric complexes formed by sodium poly(α,L-glutamate) and oppositely charged surfactants, Langmuir 12 (1996) 2169–2172.

[25] G. Pérez-Camero, M. García-Álvarez, A. Martínez De Ilarduya, C. Fernández, L. Campos, S. Muñoz-Guerra, Comblike complexes of bacterial poly(γ,D-glutamic acid) and cationic surfactants, Biomacromolecules 5 (2004) 144–152.

[26] M. García-Álvarez, J. Álvarez, A. Alla, A. Martínez De Ilarduya, C. Herranz, S. Muñoz-Guerra, Comb-like ionic complexes of cationic surfactants with bacterial poly(γ-glutamic acid) of racemic composition, Macromol. Biosci. 5 (2005) 30–38.

[27] A. Tolentino, A. Alla, A. Martínez De Ilarduya, S. Muñoz-Guerra, Comb-like ionic complexes of pectinic and alginic acids with alkyltrimethylammonium surfactants, Carbohydr. Polym. 86 (2011) 484–490.

[28] A. Gamarra, A. Martínez De Ilarduya, M. Vives, J. Morató, S. Muñoz-Guerra, Ionic complexes of poly(γ-glutamic acid) with alkyltrimethylphosphonium surfactants, Polymer 116 (2017) 43–54.

[29] V. Muriel-Galet, M.J. Cran, S, W, P. Bigger, P. Hernández-Muñoz, R. Gavara, Antioxidant and antimicrobial properties of ethylene vinyl alcohol copolymer films based on the release of oregano essential oil and green tea extract components, J. Food Eng. 149 (2015) 9–16.

[30] J.A. Alkrad, Y. Mrestani, D. Stroehl, S. Wartewig, R. Neubert, Characterization of enzymatically digested hyaluronic acid using NMR, Raman, IR, and UV–Vis spectroscopies, J. Pharm. Biomed. Anal. 31 (2003) 545–550.

[31] R. Gilli, M. Kacuráková, M. Mathlouthi, L. Navarini, S. Paoletti, FTIR studies of sodium hyaluronate and its oligomers in the amorphous solid phase and in aqueous solution, Carbohydr. Res. 263 (1994) 315–326.

[32] G. Witschard, C.E. Griffin, Infrared absorption characteristics of alkyl and aryl substituted phosphonium salts, Spectrochim. Acta 19 (1963) 1905–1910.

[33] M.A.A. Beg, Samiuzzaman, spectroscopic studies of organophosphorus compounds–II : infrared and ultraviolet spectra of phosphonium compounds and their structures, Tetrahedron 24 (1968) 191–198.

[34] A. Kanazawa, O. Tsutsumi, T. Ikeda, Y. Nagase, Novel thermotropic liquid crystals without a rigid core formed by amphiphiles having phosphonium ions, J. Am. Chem. Soc. 119 (1997) 7670–7675.

[35] J.A. Portilla-Arias, M. García-Alvarez, A. Martínez De Ilarduya, S. Muñoz-Guerra, Thermal decomposition of microbial poly(γ-glutamic acid) and poly(γ-glutamate) s, Polym. Degrad. Stab. 92 (2007) 1916–1924.

[36] M.B. Caspersen, J.P. Roubroeks, Q. Liu, S. Huang, J. Fogh, R. Zhao, K. Tømmeraas, Thermal degradation and stability of sodium hyaluronate in solid state, Carbohydr. Polym. 107 (2014) 25–30.

[37] K.M. Lowry, E.M. Beavers, Thermal stability of sodium hyaluronate in aqueous solution, J. Biomed. Mater. Res. 28 (1994) 1239–1244.

[38] E.F. Jordan, D.W. Feldeisen, A.N. Wrigley, Side-chain crystallinity. I. Heats of fusion and melting transitions on selected homopolymers having long side chains, J. Polym. Sci. Part A-1 Polym. Chem. 9 (1971) 1835–1851.

[39] M.G. Broadhurst, An analysis of the solid phase behavior of the normal paraffins, Phys. Chem. 66A (3) (1962) 241–249.

[40] D.C. West, I.N. Hampson, F. Arnold, S. Kumar, Angiogenesis induced by degradation products of hyaluronic acid, Science 228 (1985) 1324–1326.

[41] M. Vaara, Agents that increase the permeability of the outer membrane, Microbiol. Rev. 56 (1992) 395–411.